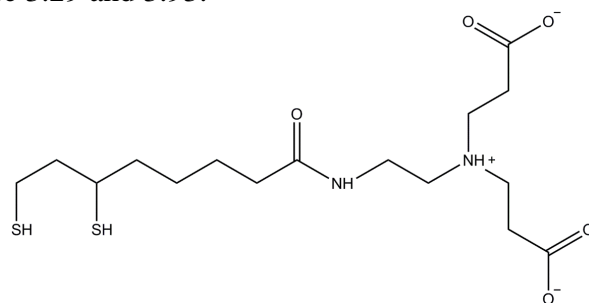Supporting Information:

Enhancing Coupled Enzymatic Activity by Conjugating One Enzyme to a Nanoparticle

*James N. Vranish, Mario G. Ancona, Eunkeu Oh, Kimihiro Susumu, and Igor L. Medintz*

Table of Contents

Supplementary Figure 1. Structure of CL4 ligands. The pI of the ammonium group is 9.06 and the carboxylate groups are 3.29 and 3.93.[1]

Supplementary Figure 2. Effect of TMB concentration on the kinetics of HRP. The activity of HRP (1 nM) was measured at various concentrations of TMB using 1 mM H_2O_2 as a substrate.
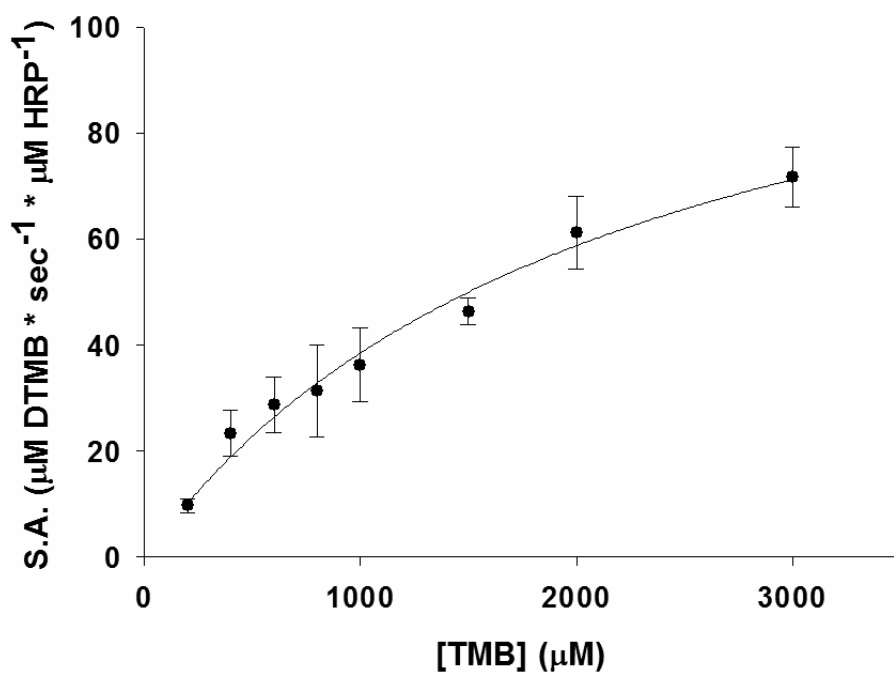
Supplementary Figure 3. HRP (1 nM), either with or without 2 equivalents of 520 QD, was incubated in a reaction mixture containing a final concentration of 1 mM TMB at 30 $^{\circ}$C for varying lengths of time prior to initiation of the reaction by the addition of 1 mM H_2O_2. The initial kinetics were recorded and plotted.
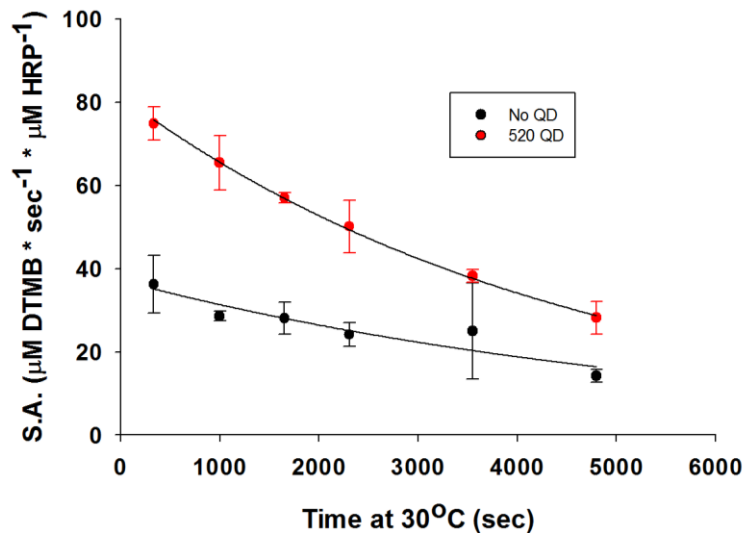
Supplementary Figure 4. Effect of buffers, pH, and salt concentration on the QD-dependent rate enhancement of HRP. Rate enhancement was calculated as the ratio of initial rates for samples containing 2 equivalents of 520 QD per HRP to the rate of HRP lacking QD.
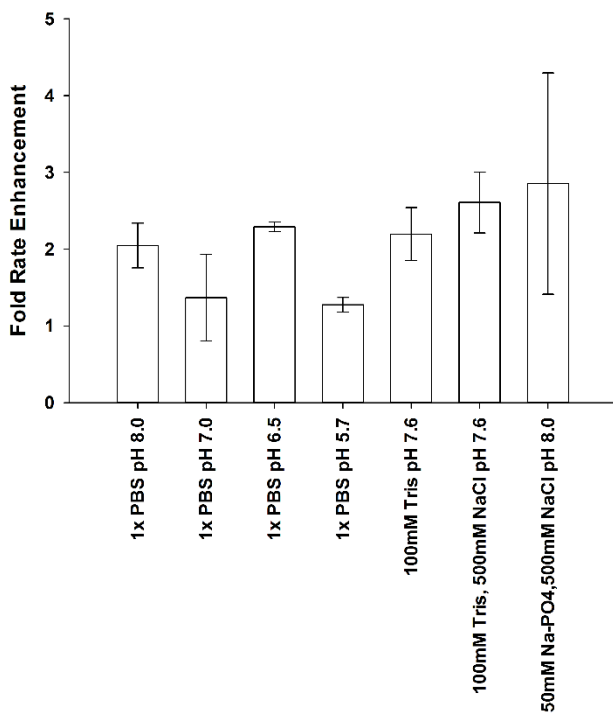
COPASI Modeling of HRP Inactivation by H_2O_2.

Modeling Methods
   The kinetics of HRP at H_2O_2 concentrations of >1 mM were modeled using a dead-end inhibition model. The parameter estimation function of COPASI kinetic modeling software was used to obtain rate constants for the modeled reactions. The inhibition of HRP was modeled using reactions SC1 (Supplementary COPASI 1) and SC2.

$SC1$) $H_2O_2 + HRP + TMB \rightarrow HRP + DTMB$

$SC2$) $HRP + H_2O_2 \rightarrow HRP_{Inactive}$
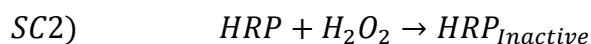
The HRP reaction was modeled using equation SC3. In these studies the K_M values for equation SC3 were fixed to the values derived from the Michaelis-Menten fits at lower H_2O_2 concentrations. The inactivation mechanism was modeled in one of two ways (equations SC4a and SC4b). Equation SC4a was eventually used to obtain the inactivation rate constant for the reactions.

$SC3$) $v = \dfrac{[H_2O_2] \times [HRP] \times k_{cat}}{K_M + [H_2O_2]}$

$SC4a$) $v_{Inactivation} = k_{Inactivate} \times [H_2O_2] \times [HRP]$

$SC4b$) $v_{Inactivation} = \dfrac{[H_2O_2] \times [HRP] \times k_{Inactivate}}{K_M^{Inactivate} + [H_2O_2]}$

For the parameter estimation, the initial concentration of DTMB was set to the concentration for each sample at time 0, to allow for some initial formation of product prior to initiation of data collection. The initial concentration of HRP and TMB were set to 1 nM and 1 mM respectively and were allowed to vary during the course of the reaction. The values for k_{cat} and $k_{inactivate}$ were limited to < 1000 sec^{-1} and $< 10^6$ M^{-1}sec^{-1} respectively. The values were minimized using a directed evolution algorithm and $> 200,000$ functions were evaluated until the fit appeared to have ceased minimizing.

Parameter Scans with Copasi
A parameter scan of $K_M^{Inactivate}$ was generated using Copasi software. The reaction and inhibition of HRP was modeled using equations SC3 and SC4b. $K_M^{Inactivate}$ was stepped from 10^3 to 10^6 µM in a logarithmic fashion with 15 data points. The sum of the squares of the error was plotted for each $K_M^{Inactivate}$ value following a directed evolution minimization of 100,000 functions for each data point.

Supplementary Figure 5. Modeling of inactivation rates of HRP. Raw data for the formation of TMB radicals at varying concentrations of H_2O_2 in the absence of QD (A) and presence of 2 equivalents of 520 QD (B). Solid lines represent the best fit from data simulations (parameters are in Table S1). H_2O_2 concentrations that were used were 1mM (grey), 2mM (black), 4 mM (red), 6 mM (blue), 10 mM (pink), 20 mM (cyan), 36 mM (yellow), and 50 mM (green).
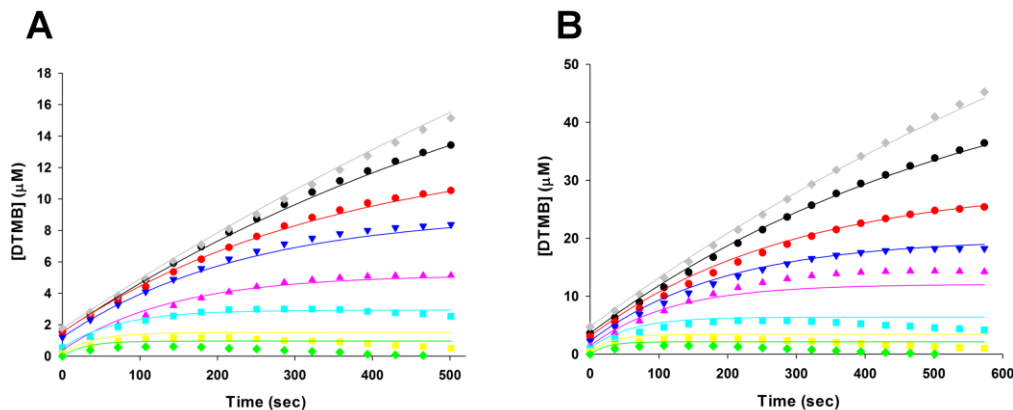
Table S1. Reaction parameters for HRP derived from H_2O_2 inhibition studies in Figure S4.

Kinetic parameters derived from H_2O_2 inhibition studies

|	k_{cat} (sec^{-1})	K_M (μM)	$k_{inactivate}$ (M^{-1} sec^{-1})
No QD	33.7 ± 0.3	27[1]	0.70 ± 0.01
520 QD	90.9 ± 0.8	28[1]	0.85 ± 0.02

[1]Values were fixed during the parameter optimization.

Supplementary Figure 6. Plots of the sum of squares error vs. $K_M^{\text{Inactivation}}$ values for H_2O_2 inactivation. Plots were generated for HRP bound to 520 QD (black) and no QD (red). This demonstrates that the inactivation can be modeled without a Michaelis complex as in Figure S4 and Table S1.
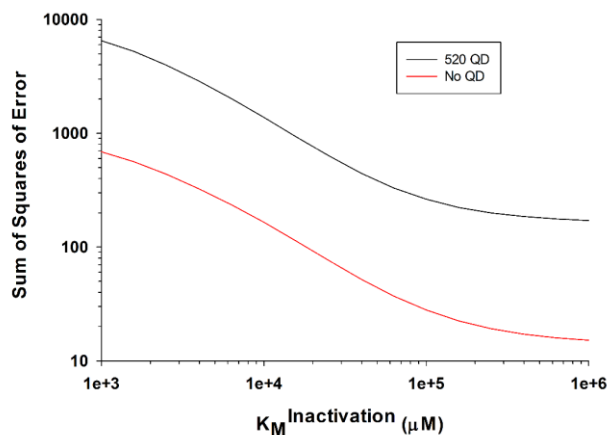
Supplementary Figure 7. Effect of QD loading ratio on the activity of HRP when using glucose and GOX as H_2O_2 generators. HRP (1 nM) was incubated with varying ratios of either 520 QD (open circles) or 655 QD (filled circles). The activity was measured using 20 mM glucose combined with 10 nM GOX as the hydrogen peroxide source. The observed rates were compared to identical samples lacking QDs.
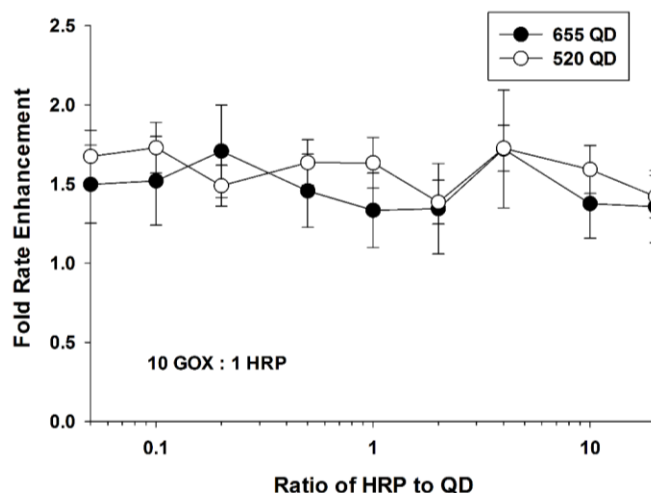
Supplementary Figure 8. Rapid kinetics modeling of the oxidation of TMB over time. The red dashed line highlights how peroxide inhibition will begin to be significant at longer time points (>30 sec), which is consistent with the delay time between peroxide addition and the start of our kinetic assays.
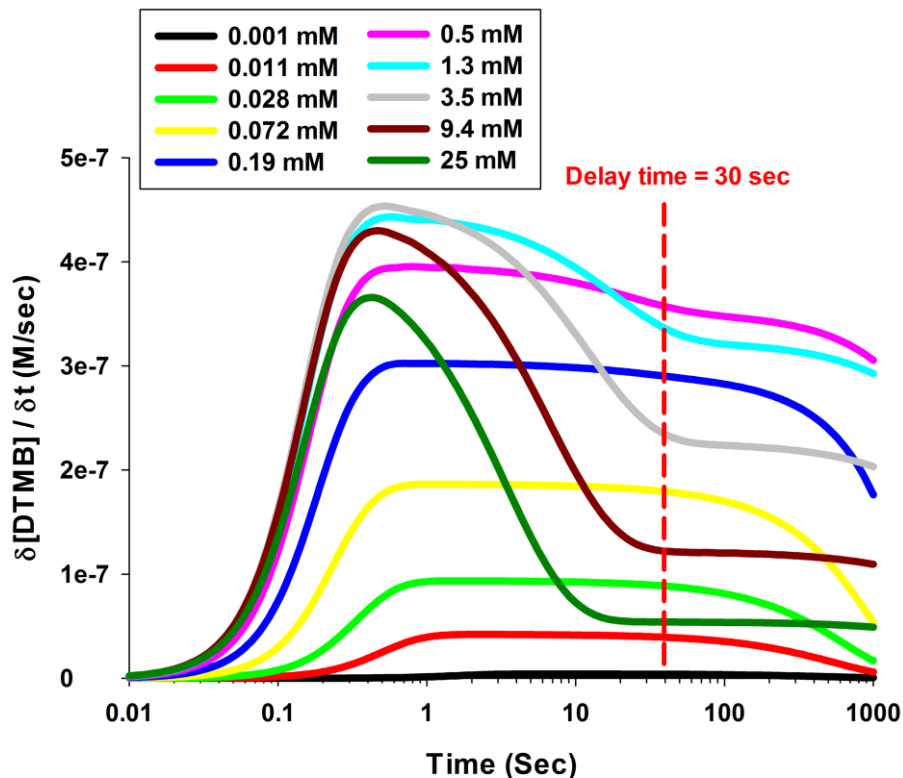
Modeling of the kinetics of HRP and GOX.

Kinetic Equations

Letting $g_{red} \equiv [G_{red}]$, $g_{ox} \equiv [G_{ox}]$, $s \equiv [S]$, $o \equiv [O_2]$, $p \equiv [H_2O_2]$, $h \equiv [HRP]$, $h_1 \equiv [HRP_I]$, $h_2 \equiv [HRP_{II}]$, $m \equiv [TMB]$, $m^* \equiv [TMB^*]$, and $m_d \equiv [TMB:TMB]^*$, and assuming well-stirred conditions, then the kinetics of the ideal reactions (1a-c) and (3) will be governed by the ordinary differential equations (ODE):

(S1a) $\qquad \dfrac{dg_{ox}}{dt} = k_o g_{red} o - k_r g_{ox} s \qquad \dfrac{ds}{dt} = -k_r g_{ox} s \qquad \dfrac{dp}{dt} = k_o g_{red} o - k_1 hp$

(S1b) $\qquad \dfrac{dh}{dt} = k_3 h_2 m - k_1 hp \qquad \dfrac{dh_1}{dt} = k_1 hp - k_2 h_1 m \qquad \dfrac{dm}{dt} = -k_2 h_1 m - k_3 m h_2$

(S1c) $\qquad \dfrac{dm^*}{dt} = k_2 h_1 m + k_3 h_2 - k_4 m^* m \qquad m_{tot} \equiv [TMB_{tot}] = m + m^* + 2m_d$

(S1e) $\qquad g_{tot} \equiv [G_{tot}] = g_{ox} + g_{red} \qquad h_{tot} \equiv [HRP_{tot}] = h + h_1 + h_2$

S8

Taking o, g_{tot}, h_{tot}, m_{tot}, and the various reaction rates as known, then the system in (S1) represent 10 equations in 10 unknowns that, with proper initial conditions imposed (including that $p(t = 0) = p_{init}$), can be solved for all variables including the main observable m_d. Numerically, the wide range of concentrations involved (e.g., $h_{tot} \sim 1$ nM while p can be as large as 20 mM) implies a stiff system and an appropriate ODE solver should be used, especially as p gets larger.

Generalizing the ideal system by using (2a) and (2b) instead of (1b) requires introducing the additional variables $m_1 \equiv [HRP_I:TMB]$, and $m_2 \equiv [HRP_{II}:TMB]$. Furthermore, if the side reactions (4)-(6) are to be included, then other needed variables are $h_3 \equiv [HRP_{III}]$, $h_4 \equiv [P670]$, $p_1 \equiv [HRP_I:H_2O_2]$, $p_2 \equiv [HRP_{II}:H_2O_2]$, $m_a \equiv [QD:TMB]$, $g_{sq} \equiv [G_{sq}]$, $g_{redt} \equiv [G_{red}:DTMB]$, $g_{sqt} \equiv [G_{sq}:DTMB]$, and $q \equiv [QD]$, and the system of ODEs becomes:

$$(S2a) \qquad \frac{dg_{ox}}{dt} = k_{o4}g_3 - k_r g_{ox}s + k_{p12}g_{sqt} \qquad \frac{dg_{sq}}{dt} = k_{p10}g_{redt} - k_{-p9}g_{redt}$$

$$(S2b) \qquad \frac{dg_{red}}{dt} = -k_{o1}g_{red}o + k_{-o1}g_1 + k_r g_{ox}s - k_{p9}g_{red}m_d + k_{-p9}g_{redt}$$

$$(S2c) \quad \frac{ds}{dt} = -k_r g_{ox}s \qquad \frac{dp}{dt} = k_{o4}g_3 - k_1 hp - k_{p2}h_1 p + k_{-p2}p_1 - k_{p6}h_2 p + k_{-p6}p_2$$

$$(S2d) \quad \frac{dp_1}{dt} = k_{p2}h_1 p - (k_{-p2} + k_{p3} + k_{p4} + k_{p5})p_1 \qquad \frac{dp_2}{dt} = k_{p6}h_2 p - (k_{-p6} + k_{p7})p_2$$

$$(S3e) \qquad \frac{dg_{redt}}{dt} = k_{p9}g_{red}m_d - (k_{-p9} + k_{p10})g_{redt}$$

$$(S2f) \qquad \frac{dh}{dt} = k_{3b}m_2 - k_1 hp + k_{p3}p_1 + k_{p8}h_3 + k_{p10b}c_2 \qquad \frac{dh_3}{dt} = k_{p7}p_2 - k_{p8}h_3$$

$$(S2g) \quad \frac{dh_1}{dt} = k_1 hp - k_{2a}h_1 m + k_{-2a}m_1 - k_{p2}h_1 p + k_{-p2}p_1 + k_{p9a}h_1 g_1 - k_{-p9a}c_1$$

$$(S2h) \quad \frac{dh_2}{dt} = k_{2b}m_1 - k_{3a}h_2 m + k_{-3a}m_2 + k_{p4}p_1 - k_{p6}h_2 p + k_{-p6}p_2 + k_{p10a}h_2 g_1$$

$$-k_{-p10a}c_2 + k_{p9b}c_1$$

$$(S2i) \qquad \frac{dm}{dt} = -k_{2a}h_1 m + k_{-2a}m_1 - k_{3a}h_2 m + k_{-3a}m_2 - k_{p1}qm + k_{-p1}m_a$$

$$(S2j) \qquad \frac{dm_1}{dt} = k_{2a}mh_1 - (k_{-2a} + k_{2b})m_1 \qquad \frac{dm_2}{dt} = k_{3a}mh_2 - (k_{-3a} + k_{3b})m_2$$

$$(S2k) \qquad \frac{dm^*}{dt} = k_{2b}m_1 + k_{3b}m_2 - k_4 m^* m \qquad \frac{dm_d}{dt} = k_4 m^* m$$

$$(S2l) \qquad m_{tot} = m + m^* + m_a + 2m_d + m_1 + m_2 + 2g_{redt} + 2g_{sqt}$$

$$(S2m) \qquad g_{tot} == g_{ox} + g_{red} + g_{sq} + g_{redt} + g_{sqt} \qquad q_{tot} = q + m_a$$

$$(S2n) \qquad h_{tot} = h + h_1 + h_2 + h_3 + h_4 + m_1 + m_2 + p_1 + p_2$$

The system now consists of 21 equations in 21 unknowns which can be solved if proper initial conditions are given and all parameters are known. Although some of the rate constants are given in the literature, we generally use our own values since the conditions in our experiments are unavoidably different from published work; however, in no case are our values substantially different from published ones.

Justification of Michaelis-Menten in the Ideal Case.

The ideal HRP system of equations in (S1) can be reduced to a formula for dm_d/dt of the Michaelis-Menten form if one assumes $m \cong m_{tot}$, that the k_4 reaction is fast, neglects the k_5 reaction, and invokes "Briggs-Haldane"-like assumptions, namely that $dh/dt \cong dh_1/dt \cong 0$. The result is:

$$(S3a) \qquad\qquad V \equiv \frac{dm_d}{dt} \cong \frac{k_{cat}^* h_{tot} p}{K_M^* + p}$$

$$(S3b) \qquad \text{where} \qquad k_{cat}^* = \frac{2k_2 k_3 m_{tot}}{k_2 + k_{23}} \qquad K_m^* = \frac{k_{cat}^*}{2k_1} = \frac{k_2 k_3 m_{tot}}{k_1(k_2 + k_3)}$$

This is confirmed by simulation with the parameters given in Table 1 and the plot in Fig. 3C. That the ideal equations fit the data well suggests that the side reactions are unimportant in this regime.

Hydrogen Peroxide Production by GOX.

To assess the potential for hydrogen peroxide inhibition occurring in the GOX-HRP experiments, we simulate the H_2O_2 production for various levels of glucose and delay time, assuming [GOX] = 20 nM. For these calculations, we use the GOX kinetic parameters of Gibson *et al.*[2] The result is plotted in Figure S9, and from this plot we see that under all circumstances considered in this paper, the H_2O_2 concentration always remains below 1 mM. Based on the experiments of Figure 6, we therefore expect H_2O_2 inhibition to not be an important contributor to the GOX-HRP experiments, and specifically the inhibition effect seen in Fig. 6D.

Table S2. Reaction parameters for HRP side reactions.

| HRP kinetic parameters for side reactions		
Rate constant	Literature[3-4]	This work
k_{p1} (M^{-1}sec^{-1})	---	5×10^5
k_{-p1} (sec^{-1})	---	0.07
k_{p2} (M^{-1}sec^{-1})	500	500
k_{-p2} (sec^{-1})	Slow	0.46
k_{p3} (sec^{-1})	1.76	1.76
k_{p4} (sec^{-1})	0.0079	0.0079
k_{p5} (sec^{-1})	0.0039	0.0039
k_{p6} (M^{-1}sec^{-1})	25	25
k_{-p6} (sec^{-1})	Slow	0.04
k_{p7} (sec^{-1})	0	0
k_{p8} (sec^{-1})	0.0022	0.0022
$k_{p9} = k_{p11}$ (M^{-1}sec^{-1})	---	3×10^9
$k_{-p9} = k_{-p11}$ (sec^{-1})	---	50
$k_{p10} = k_{p12}$ (sec^{-1})	---	1000

Supplementary Figure 9. Simulated levels of hydrogen peroxide as produced by GOX with glucose as a substrate following a delay time of either 30 or 100 seconds.
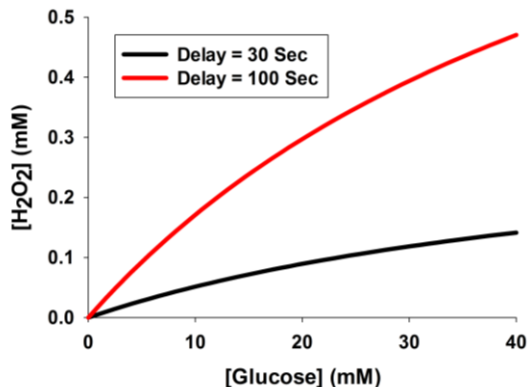
Supplementary Figure 10. Bleaching of TMB charge transfer complex by GOX/glucose or H_2O_2. Reactions were set up with 2 nM HRP, 500 uM H_2O_2, 1 mM TMB, and 20 mM glucose. Once the absorbance at 650 nm had nearly maximized, either 20 mM H_2O_2 or 370 nM GOX was added. An additional control was run that received no additional component.
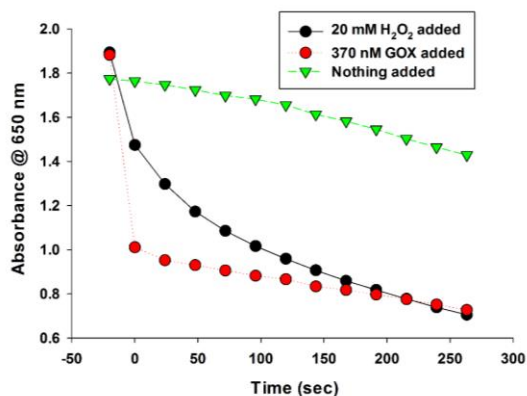
Supplementary Figure 11. Light exposure doesn't affect HRP kinetics on QD. HRP was bound to 2 equivalents of 520 QD at a final concentration of 1 nM. The reactions contained 1 mM TMB and were initiated simultaneously by the addition of 1 mM H_2O_2 within a dark plate reader. The reactions shown in black were monitored immediately while those in red and green were kept in the dark for 141 sec and 281 sec respectively prior to initiating light exposure and reaction monitoring.
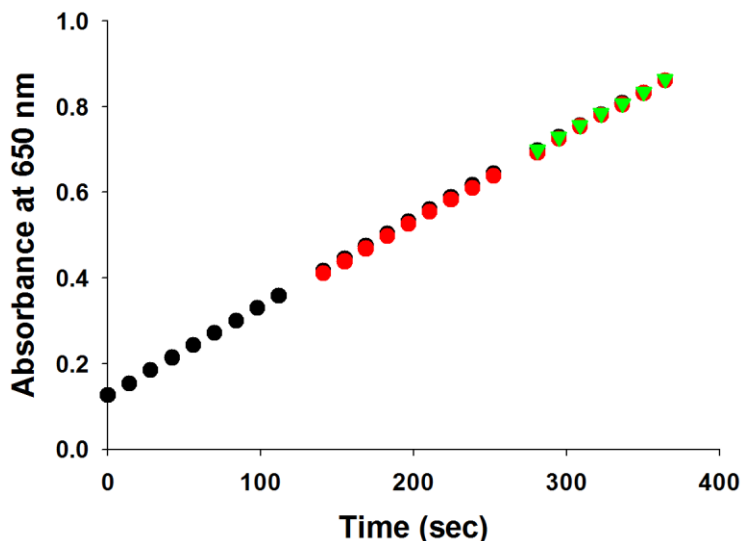
REFERENCES

1.   Susumu, K.; Oh, E.; Delehanty, J. B.; Blanco-Canosa, J. B.; Johnson, B. J.; Jain, V.; Hervey, W. J.; Algar, W. R.; Boeneman, K.; Dawson, P. E.; Medintz, I. L., Multifunctional Compact Zwitterionic Ligands for Preparing Robust Biocompatible Semiconductor Quantum Dots and Gold Nanoparticles. *J Am Chem Soc* **2011,** *133* (24), 9480-9496.
2.   Gibson, Q. H.; Massey, V.; Swoboda, B. E. P., Kinetics + Mechanism of Action of Glucose Oxidase. *J Biol Chem* **1964,** *239* (11), 3927-&.
3.   Arnao, M. B.; Acosta, M.; del Rio, J. A.; Garcia-Canovas, F., Inactivation of peroxidase by hydrogen peroxide and its protection by a reductant agent. *Biochim Biophys Acta* **1990,** *1038* (1), 85-9.
4.   Arnao, M. B.; Acosta, M.; del Rio, J. A.; Varon, R.; Garcia-Canovas, F., A kinetic study on the suicide inactivation of peroxidase by hydrogen peroxide. *Biochim Biophys Acta* **1990,** *1041* (1), 43-7.